

# Experimental evidence for competition between antiferromagnetic and ferromagnetic correlations in $\text{HgCr}_2\text{S}_4$

V. Tsurkan,<sup>1,2</sup> J. Hemberger,<sup>1</sup> A. Krimmel,<sup>1</sup> H.-A. Krug von Nidda,<sup>1</sup> P. Lunkenheimer,<sup>1</sup> S. Weber,<sup>1</sup> V. Zestrea,<sup>2</sup> and A. Loidl<sup>1</sup>

<sup>1</sup>*Experimental Physics V, Centre for Electronic Correlations and Magnetism, University of Augsburg, D-86159 Augsburg, Germany*

<sup>2</sup>*Institute of Applied Physics, Academy of Sciences of Moldova, MD-2028, Chişinău, R. Moldova*

(Received 22 December 2005; revised manuscript received 10 March 2006; published 30 June 2006)

A detailed study of polycrystalline and single crystalline samples of the normal spinel  $\text{HgCr}_2\text{S}_4$  is reported. The structural refinement reveals enhanced values of the atomic displacements suggesting the closeness to a structural instability. Magnetization, electron-spin resonance, and specific-heat studies document strong ferromagnetic fluctuations close to 50 K and the occurrence of complex antiferromagnetic order at  $T_N=22$  K. We found highly unconventional behavior resembling properties of a noncollinear antiferromagnet and of a soft ferromagnet dependent on temperature and magnetic field. Even weak external magnetic fields disturb the antiferromagnetic order and strongly enhance the ferromagnetic correlations. The observed anomalies are related to bond frustration due to competing magnetic exchange interactions between the Cr ions.

DOI: [10.1103/PhysRevB.73.224442](https://doi.org/10.1103/PhysRevB.73.224442)

PACS number(s): 75.30.Cr, 75.40.Cx, 76.30.-v, 76.50.+g

## I. INTRODUCTION

Magnetic compounds with frustrated exchange due to geometric constraints became the subject of current theoretical and experimental interest. Transition-metal oxides and chalcogenides with the general formula  $AB_2X_4$  exhibiting the spinel structure received special attention. In  $AB_2X_4$  spinels both cation sites, the tetrahedrally coordinated  $A$  site and the octahedrally coordinated  $B$  site, are geometrically frustrated. The  $A$  sites form two interpenetrating *fcc* lattices, while the  $B$  sites constitute a pyrochlore lattice with corner sharing tetrahedra. In addition, many magnetic spinel compounds are governed by another type of frustration that so far has not been studied in detail. Depending on the lattice constant, nearest neighbor (NN) direct antiferromagnetic (AFM)  $B$ - $B$  exchange and indirect NN ferromagnetic  $90^\circ$  (FM)  $B$ - $X$ - $B$  superexchange via anions are competing in the oxide spinels.<sup>1</sup> In the chalcogenide spinels, the direct AFM exchange is weakened by the larger intercation distance, but more-distant neighbor antiferromagnetic superexchange interactions like  $B$ - $X$ - $A$ - $X$ - $B$  or  $B$ - $X$ - $X$ - $B$  become important.<sup>2-4</sup> There are cases when the competing interactions are equal and almost cancel each other, revealing Curie-Weiss (CW) temperatures close to zero, a situation characterized as bond frustration. So far it is unclear whether geometrical frustration and bond frustration drive similar exotic ground states. It is a common belief that the phenomena recently found in magnetic spinels, e.g., heavy-fermion-like liquid states,<sup>5-7</sup> spin-singlet states,<sup>8,9</sup> composite spin degree of freedom,<sup>10</sup> spin-orbital liquid and orbital glass states,<sup>11-14</sup> as well as the colossal magneto-capacitive coupling in spinel multiferroics,<sup>15,16</sup> bear the sign of the geometrical frustration that enhances the spin, orbital, and lattice fluctuations. Besides the pure academic interest, this fascinating physics offers new possibilities for spintronic applications and the design of devices with advanced functionality.

Most chalcogenide chromium spinels  $A\text{Cr}_2X_4$  (with  $A = \text{Cd}, \text{Hg}$ ;  $X = \text{S}, \text{Se}$ ) are simple Heisenberg ferromagnets,<sup>17</sup> and hence are not expected to be geometrically frustrated.

However,  $\text{HgCr}_2\text{S}_4$  shows a noncollinear AFM order despite a high positive CW temperature of 142 K dominated by a strong FM exchange.<sup>3</sup> Neutron-diffraction investigations at low temperatures and in zero magnetic field revealed a spiral spin configuration.<sup>18</sup> Moderate fields of only several kOe destroy the spiral structure and align the spins ferromagnetically. Early magnetization measurements report a Curie temperature of 36 K,<sup>4</sup> but disagree with the results of neutron diffraction<sup>18</sup> and optical<sup>19</sup> studies, which conclude that  $\text{HgCr}_2\text{S}_4$  is an antiferromagnet below a critical temperature of 60 K. The reason for this discrepancy remained unclear.

The scope of our study was to reveal the magnetic, electronic, and thermal correlations in a compound with chromium ions occupying solely  $B$  sites of the intrinsically frustrated pyrochlore lattice. This lattice is known to preclude a simple AFM spin arrangement.<sup>20,21</sup> Indeed,  $\text{HgCr}_2\text{S}_4$  manifests a complex AFM ground state, however, the FM exchange interactions are strong and dominating. Hence, we expect that bond frustration is of utmost importance here. To get information on local and macroscopic magnetic properties we used complementary techniques of dc magnetization, ac susceptibility, electron-spin resonance (ESR), and specific heat.

## II. EXPERIMENTAL DETAILS

Polycrystalline  $\text{HgCr}_2\text{S}_4$  samples were prepared by solid-state reaction from high purity (99,999%) binary mercury sulfide and elementary Cr and S in evacuated quartz ampoules. The synthesis was repeated several times in order to reach good homogeneity and to minimize nonreacted binary sulfides. The final heat treatment was performed at 800 °C in an atmosphere of sulfur excess. Such prepared polycrystals were used as a starting material for the single-crystal growth. Single crystals were obtained by a chemical transport reaction method using chlorine as a transport agent. The growth experiments were performed at temperatures between 850 and 800 °C. The crystals were obtained in a form of nearly

perfect octahedra with shiny surfaces and dimensions up to 2 mm on the edge.

Powder x-ray diffraction was performed utilizing Cu  $K_{\alpha}$  radiation with a wavelength  $\lambda=1.5406$  Å and a position-sensitive detector. The magnetization measurements were done employing a commercial superconducting quantum interference device (SQUID) magnetometer (MPMS-5, Quantum Design) in fields up to 50 kOe. The heat capacity was measured using a physical properties measurement system (PPMS, Quantum Design) in the temperature range 2 K  $< T < 300$  K and in magnetic fields up to 70 kOe. The ESR measurements were carried out with a Bruker ELEXSYS E500 CW spectrometer at X-band frequency ( $\nu=9.36$  GHz), equipped with a continuous gas-flow cryostat for helium (Oxford Instruments) covering a temperature range between 4.2 K and room temperature. For the ESR experiments thin disks with the faces along the crystallographic (110)-plane were cut from the single crystals. The disks were fixed on the sample holder allowing for rotation of the static magnetic field within the plane of the disk, where the cubic  $\langle 001 \rangle$ ,  $\langle 110 \rangle$ , and  $\langle 111 \rangle$  directions can be adjusted. The microwave field was always applied perpendicular to the plane.

### III. EXPERIMENTAL RESULTS AND DISCUSSION

#### A. Structural analysis

The structural details of powdered single crystals and polycrystals were investigated by conventional x-ray powder diffraction at room temperature. The diffraction profiles and refinements for the corresponding samples are shown in Fig. 1. The data were analyzed by standard Rietveld refinement using the FULLPROF program.<sup>22</sup>  $\text{HgCr}_2\text{S}_4$  crystallizes in the normal cubic spinel structure with space group  $Fd\bar{3}m$  (No. 227). No indications of impurity phases could be detected. In total 12 parameters have been refined: scale factor, zero-point shift, three resolution parameters, lattice parameter  $a_0$ , sulfur positional parameter  $x$  in fractional coordinates (f.c.), Hg site-occupation factor (SOF), Cr SOF factor, and three isotropic temperature factors,  $B_{\text{iso}}$ , for Hg, Cr, and S, respectively. The refined structural parameters are presented in Table I.

The refined structural parameters of single crystals and polycrystalline samples are in very good mutual agreement. As shown in the inset of Fig. 1, there is a slight redistribution of the intensity between the peaks (511) at  $2\Theta \approx 46.0^\circ$  and (440) at  $2\Theta \approx 50.4^\circ$  for polycrystals and single crystals, which indicates some difference in the cationic defect structure. Most important, large isotropic temperature factors ( $B_{\text{iso}}=8\pi^2u^2$  with  $u$  being the mean square displacement) have been found for all three constituent atoms. These isotropic temperature factors are enhanced by almost one order of magnitude as compared to the majority of other magnetic spinel compounds.<sup>23</sup> Such strongly enhanced values of the atomic displacement together with the high value of the sulfur positional parameter suggest that  $\text{HgCr}_2\text{S}_4$  is close to a structural instability.

#### B. Magnetization

Figure 2 presents the temperature dependences of the magnetization  $M$  for polycrystalline and single crystalline

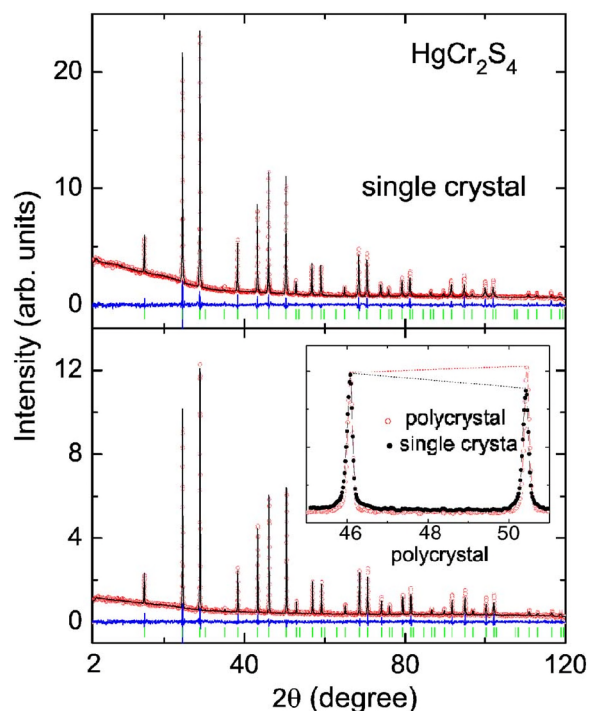


FIG. 1. (Color online) X-ray diffraction profiles of  $\text{HgCr}_2\text{S}_4$  polycrystals (lower frame) and crushed single crystals (upper frame). The measured intensities (open circles) are compared with the calculated profile using Rietveld refinement (solid line). Bragg positions of the normal cubic spinel structure are indicated by vertical bars and the difference pattern by the lower thin solid line. The inset shows the measured intensities of the (511) and (440) reflections of the single (closed circles) and polycrystalline (open circles) samples. Scaling of the (511) reflection to the same intensity results in an increase (decrease) of the (440) reflection for the polycrystalline (single crystalline) sample, respectively.

samples of  $\text{HgCr}_2\text{S}_4$  measured at different fields. At low fields ( $H \leq 1$  kOe) the magnetization shows a sharp increase at temperatures below 60 K apparently indicating the development of strong FM correlations in agreement with the earlier results.<sup>3</sup> On further decreasing temperatures the magnetization shows a maximum at about 30 K followed by a downturn resembling a transition into an AFM state. The maximum in  $M$  is shifted to lower temperatures with increasing magnetic fields indicating the suppression of the AFM state. It finally disappears in fields above 10 kOe, where the magnetization monotonously increases with decreasing temperature. We note a strong enhancement of the ferromagnetic correlations by the magnetic field. The determination of the transition temperature as routinely performed for ferromagnets by plotting  $(dM/dT)/M$  vs  $T$  yields a value of about 50 K for measurements in a field of 100 Oe. However, we will show below that this is not a temperature that marks the onset of long-range FM order but indicates the appearance of strong FM correlations. For an external field of 50 kOe, the transition temperature increases up to 100 K. Although in the latter case the FM order is not strictly defined, such a strong shift of the effective transition towards higher temperatures induced by a magnetic field is probably the largest one ever reported for a ferromagnetic compound. Already at this point

TABLE I. Crystallographic data on  $\text{HgCr}_2\text{S}_4$  crystals.

Sample	$a_0$ (Å)	$x(\text{S})$ (f.c.)	SOF (Hg)	SOF (Cr)	$B_{\text{iso}}(\text{Hg/Cr/S})$ (Å <sup>2</sup> )	$R_{\text{Bragg}}$
SC	10.256(1)	0.267(1)	1.08(3)	1.02(3)	2.2(1)/1.8(2)/2.3(3)	5.7%
PC	10.252(1)	0.265(1)	1.05(3)	1.07(3)	2.3(1)/2.5(2)/1.8(3)	4.3%

we note that strong ferromagnetic correlations are present in  $\text{HgCr}_2\text{S}_4$  at about 50 K, although the ground state is a complex antiferromagnet. Similar observations have been reported in doped manganites and were interpreted as driven by the competition of charge, spin, and orbital degrees of freedom. But we would like to recall that in  $\text{HgCr}_2\text{S}_4$  the  $3d$  electrons of the Cr ions are rather orbitally inactive due to the half-filled  $t_{2g}$  shell. Beside this, all Cr ions are in a  $3+$  state. Thus, the variation of the magnetic state in  $\text{HgCr}_2\text{S}_4$  must be fully related to the spin degree of freedom.

In the inset of Fig. 2 the temperature dependence of the reciprocal susceptibility  $\chi^{-1}$  measured in a field of 10 kOe is plotted both for polycrystalline and single crystalline samples. A linear fit to the experimental data at high temperatures yields a CW temperature  $\Theta_{\text{CW}}=140$  K and an effective magnetic moment  $p=3.90\mu_B$ . The latter value agrees well with the theoretical spin-only value of  $3.87\mu_B$  for  $\text{Cr}^{3+}$  resulting from a  $3d^3$  state. The large positive value of  $\Theta_{\text{CW}}$  reflects the dominance of FM interactions in the magnetic exchange.  $\text{HgCr}_2\text{S}_4$  seems to be the only sulfo-spinel characterized by such a large positive CW temperature but revealing long-range AFM ordering at low temperatures.

Figure 3(a) shows the field dependent magnetization  $M$  at several temperatures for single crystalline  $\text{HgCr}_2\text{S}_4$  measured along the  $\langle 001 \rangle$  cube edge. According to neutron diffraction results the propagation vector of the magnetic spiral is directed along one of the cube edges in a given domain.<sup>18</sup> On decreasing temperature, in the range  $60 \text{ K} > T > 30 \text{ K}$ , the

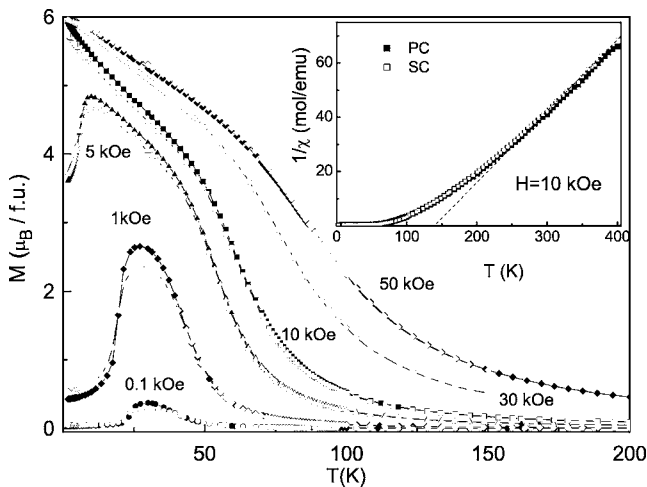


FIG. 2. Temperature dependences of the magnetization  $M$  at different fields for  $\text{HgCr}_2\text{S}_4$  polycrystals (closed symbols) and single crystals (open symbols). Inset: The temperature dependence of the reciprocal susceptibility  $\chi^{-1}$  for the same samples measured in a field of 10 kOe. The dashed line indicates a Curie-Weiss behavior of  $\chi^{-1}$ .

magnetization shows a ferromagneticlike behavior with a linear increase at low fields due to a demagnetization effect and saturation in higher fields. Below the AFM transition at  $T_N=22$  K (deduced from the specific heat data; see Sec. III D), the magnetization after zero field cooling (ZFC) reveals a substantial nonlinearity in low fields as shown in detail in Fig. 3(b). After an initial linear growth up to a certain field  $H_1$  (1.7 kOe at 2 K),  $M$  shows a steeper increase in fields up to  $H_2$  (4.5 kOe), continues with a somewhat weaker slope, and approaches saturation at the full value of  $6\mu_B$  as expected for  $2\text{Cr}^{3+}$  ions (per formula unit) in fields above  $H_3$  (8 kOe). On decreasing field a hysteretic behavior appears below  $H_2$  where the magnetization continues to decrease lin-

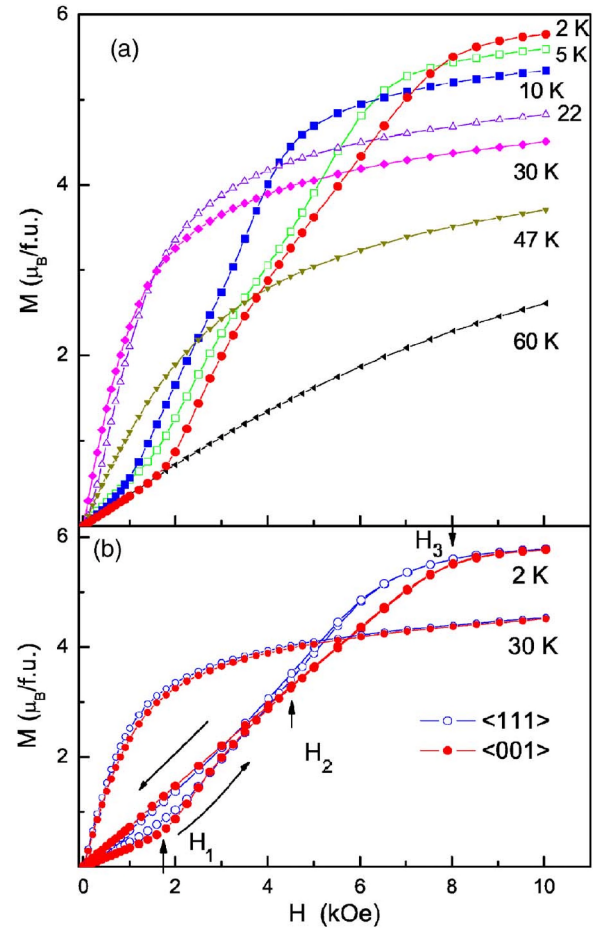


FIG. 3. (Color online) Field-dependent magnetization curves at different temperatures for  $\text{HgCr}_2\text{S}_4$  single crystals (SC): (a) for fields applied along  $\langle 001 \rangle$  direction; (b) for  $\langle 111 \rangle$  and  $\langle 001 \rangle$  directions at 2 K on an increasing and decreasing field showing hysteresis in low fields and anisotropy in saturation fields. The magnetization curves in the ferromagneticlike state at 30 K demonstrate similar demagnetization factors of the samples.

early down to zero field without any anomaly at  $H_1$ . Note that on reversing the field and repeating the full cycle the hysteresis becomes less pronounced as compared to the virgin curve. The observed hysteresis can be explained by the reorientation of the three possible domains as evidenced by neutron scattering.<sup>18</sup> No remnant magnetization was detected at any temperature proving the absence of a ferromagnetic component of the spiral in zero field. The strong increase of the saturation field  $H_3$  observed below 22 K cannot be attributed to the demagnetization field, which is of the order of 1.8 kOe for the given sample shape. The overall behavior of the magnetization measured along the  $\langle 111 \rangle$  direction is very similar to that observed along the  $\langle 001 \rangle$  axis. This suggests a very small magnetocrystalline anisotropy which is not strong enough to explain the high saturation field. Thus, the high saturation field rather has to be related to the competing exchange interactions on the gradual suppression of the spiral AFM order.

Although in the temperature range from 30 to 60 K the typical FM correlations are evident, the question arises whether they are connected with spontaneous FM order. To check this we performed a scaling analysis of the magnetization data using a technique of modified Arrott plots. We probed different critical exponents including mean field and 3D Heisenberg values. A substantial nonlinearity of the Arrott plots was present below 10 kOe in contrast to the linear behavior at high fields expected for proper ferromagnets. The nonlinearity of the Arrott plots probably again has to be related to the competition of the exchange interactions, as documented at low temperatures, the same field of 10 kOe is necessary to suppress the noncollinear spin arrangement. Thus, the presence of spontaneous magnetization in  $\text{HgCr}_2\text{S}_4$  cannot be confirmed on the basis of magnetization experiments. From the Arrott analysis only an effective Curie temperature of about 50 K can be inferred in agreement with the above-mentioned low-field estimate. But obviously no conventional spontaneous long-range FM state is established below this temperature.

### C. AC susceptibility

The temperature dependence of the real part of the susceptibility  $\chi'$  for single crystalline  $\text{HgCr}_2\text{S}_4$ , as measured at a driving ac field of 4 Oe at different external dc magnetic fields, is presented in Fig. 4. In the absence of an external magnetic field,  $\chi'$  shows a broad maximum located at 30 K similar to the low field dc susceptibility plotted in the same figure. The steepest slope of the left wing in  $\chi' = f(T)$  in zero field occurs at 22 K and marks  $T_N$ . Application of a dc magnetic field strongly suppresses the maximum of  $\chi'$  and concomitantly shifts it to higher temperatures (right scale of Fig. 4). In the frequency range from 1 to 1000 Hz the real part  $\chi'$  of the ac susceptibility is frequency independent. The imaginary part  $\chi''$  is about two orders of magnitude smaller than the real part  $\chi'$  and, hence, is practically undetectable due to the uncertainty in phase adjustment. The behavior of the ac susceptibility for the polycrystalline sample looks very similar to that of the single crystals.

### D. Specific heat

Figure 5 shows the temperature dependence of the specific heat plotted as  $C/T$  vs  $T$  both for polycrystalline and

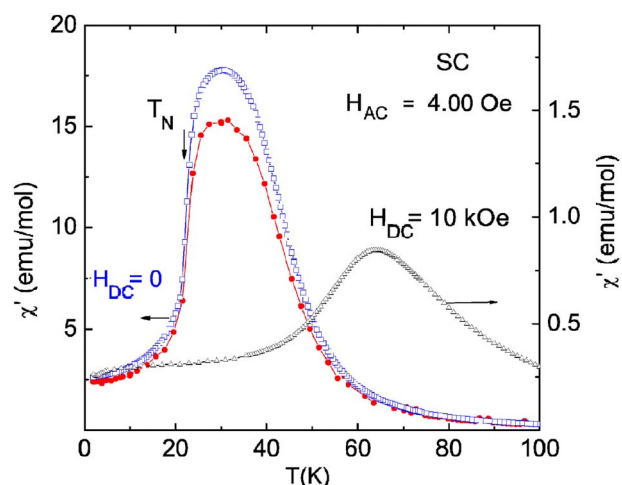


FIG. 4. (Color online) Temperature dependence of the real part of the susceptibility  $\chi'$  at two different external dc magnetic fields for single crystalline (SC)  $\text{HgCr}_2\text{S}_4$  (open symbols) compared to the dc susceptibility measured in a field of 100 Oe (closed symbols).

single crystalline  $\text{HgCr}_2\text{S}_4$ . In the single crystals the specific heat manifests a well pronounced anomaly at a temperature of 22 K (see inset of Fig. 5). This temperature coincides with the temperature  $T_N$  as determined from the ac susceptibility and is far from 50 K estimated from the dc magnetization. As documented in the inset, application of magnetic fields shifts the anomaly in the specific heat to lower temperatures indicating AFM correlations. Therefore, it can be associated with the transition into the AFM state. However, the change of the Néel temperature  $T_N$  in  $\text{HgCr}_2\text{S}_4$ , as evidenced by the specific heat data, is of several orders of magnitude higher than for conventional antiferromagnets.<sup>24–26</sup> Indeed, a field of only 1 kOe yields a huge shift of the anomaly in  $C$  down to 18 K. Concomitantly, a strong broadening of the anomaly at  $T_N$  occurs in contrast to the sharp peak seen in conven-

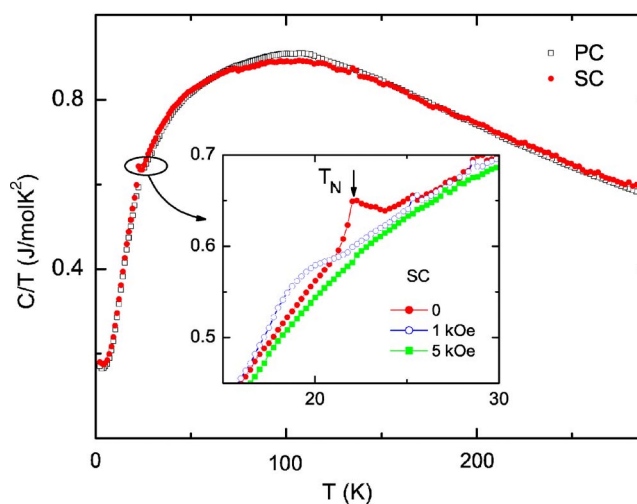


FIG. 5. (Color online) Temperature dependences of the specific heat of  $\text{HgCr}_2\text{S}_4$  plotted as  $C/T$  both for polycrystal [(PC), open symbol] and single crystal [(SC), closed symbol]. The inset represents  $C/T$  vs  $T$  at around  $T_N$  for the single crystal for different applied fields up to 5 kOe on an enlarged scale.

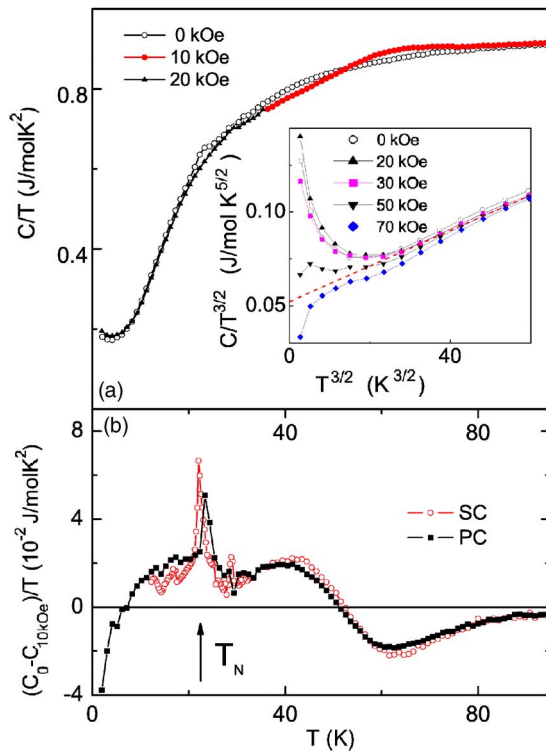


FIG. 6. (Color online) (a) Temperature dependence of the specific heat  $C/T$  in zero field and for external magnetic fields. (b) Difference between  $(C_0 - C_{10 \text{ kOe}})/T$  versus temperature for polycrystalline (PC) and single crystalline (SC) samples. Inset:  $C/T^{3/2}$  vs  $T^{3/2}$  for different applied fields at low temperatures, to estimate magnon and phonon contributions. A dashed line shows a fit to the data at zero field.

tional antiferromagnets. In fields above 5 kOe the anomaly at  $T_N$  is completely suppressed. The entropy involved in the transition calculated by integrating the difference  $(C_0 - C_{5 \text{ kOe}})/T$  over the range from 2 to 40 K sums up to  $0.35 \text{ J mol}^{-1} \text{ K}^{-1}$ . This value is surprisingly low, being only of about 1.5% of the full entropy of  $2R \ln 4$  (or  $23.12 \text{ J mol}^{-1} \text{ K}^{-1}$ ) expected for the full FM alignment of the Cr spins indicating the presence of FM fluctuations already at high temperatures.

The evolution of the specific heat at higher fields is presented in Fig. 6. At temperatures above 55 K the specific heat in finite fields becomes higher than that in zero magnetic field [Fig. 6(a)]. The difference between  $(C_0 - C_{10 \text{ kOe}})/T$  is shown on an enlarged scale in Fig. 6(b) for both polycrystals and single crystals indicating that some weight of the specific heat in the field is shifted to higher temperatures as usually observed in ferromagnets. Figure 6(b) also documents that the anomaly in the heat capacity at  $T_N$  is found to be at slightly higher temperatures in polycrystals compared to single crystals. Another feature becomes pronounced at temperatures below 9 K. In fields up to 20 kOe the specific heat is still higher than in absence of the field [see inset of Fig. 6(a)]. Together with the magnetization data in Fig. 2 this indicates an intermediate regime of competing AFM and FM correlations, where the AFM order is already broken while the FM order is not yet fully estab-

lished. Only for fields above 30 kOe the situation is reversed and the specific heat decreases as one expects for an ordinary ferromagnet, where the spin-wave dispersion opens a gap proportional to the external field. Thus, below 9 K the FM correlations in  $\text{HgCr}_2\text{S}_4$  become dominant only at high fields. To estimate the magnon contribution to the specific heat we plotted  $C/T^{3/2} = \delta + \beta_D T^{3/2}$  vs  $T^{3/2}$ , which for ferromagnets should present a straight line with slope  $\beta_D$  and intercept  $\delta$  [see inset of Fig. 6(a)]. The intercept  $\delta$  characterizes the magnon contributions and is inversely proportional to the stiffness of the magnon dispersion. The slope  $\beta_D$  is determined by the phonon part of the low-temperature specific heat and allows a direct estimate of the Debye temperature. From  $\beta_D$  a Debye temperature  $\theta_D = 240 \text{ K} \pm 5 \text{ K}$  was derived. The intercept of the linear high-temperature fits, as shown by the dashed line in the inset of Fig. 6, yields  $\delta = 0.052 \text{ J/mol K}^{5/2}$  in zero external field and decreases with increasing fields, resulting in a value of approximately  $0.04 \text{ J/mol K}^{5/2}$  for 70 kOe. This evidences the increase of the magnon stiffness on increasing external magnetic fields. Moreover, we have to mention the excess specific heat below 7 K at fields smaller than 50 kOe. It cannot be attributed to nuclear Zeeman contributions, because those should be enhanced in a magnetic field. In general, such an excess specific heat is typical for glassy states. It suggests some degree of disorder and frustration in the AFM ground state of  $\text{HgCr}_2\text{S}_4$  and the intermediate state as well. However, field-cooled and zero-field-cooled susceptibility experiments do not reveal any irreversibility which would prove some freezing process related to structural disorder. Probably strong spin fluctuations connected with the competition of FM and AFM interactions are responsible for the excess specific heat in low fields. For fields above 50 kOe the energy gap of the magnon excitations becomes evident and increases with increasing field as theoretically expected.

### E. Electron-spin resonance

Figure 7 shows the temperature evolution of the ESR spectra for the static magnetic field applied along the  $\langle 001 \rangle$  axis. Figure 8 illustrates the corresponding resonance field and linewidth. Starting at high temperatures in the paramagnetic regime, we observe a single exchange-narrowed resonance line without any orientation dependence. It can be well described by a Lorentzian shape. Its resonance field is found at 3366 Oe corresponding to a  $g$ -value  $g = 1.98$  as typically found for  $\text{Cr}^{3+}$ .<sup>27</sup> The linewidth (lower frame of Fig. 8), which is of the order of 100 Oe, first decreases on decreasing temperature, reaches a minimum of 77 Oe at 135 K and increases again up to a local maximum of 156 Oe at 60 K, which can be ascribed to critical fluctuations on approaching the ferromagneticlike transition. Note that the ESR experiments are performed in finite magnetic fields of approximately 3 kOe (see Fig. 7) which are strong enough to destroy long-range AFM order (see Fig. 2). Below 60 K the resonance field is already remarkably shifted as compared to high temperatures, but remains still isotropic under rotation of the static field within the plane of the disk. This shift is due to demagnetization fields originating from the increasing mag-

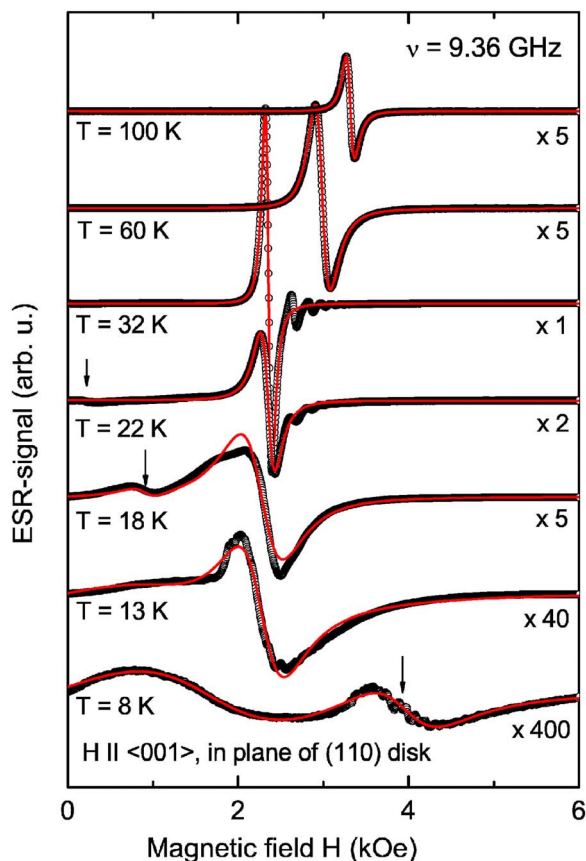


FIG. 7. (Color online) Electron-spin resonance spectra at different temperatures for thin  $\text{HgCr}_2\text{S}_4$  single crystalline disk with (110) plane orientation. The static magnetic field is applied along the  $\langle 001 \rangle$  axis. The solid lines are fits by Lorentzians, one above and two below 32 K. The arrows mark the external magnetic field for the onset of spin reorientation. The numbers on the right indicate the relative amplification factors of the ESR intensity.

netization in the disk shaped sample magnetized in plane.<sup>28</sup> On further decreasing temperature the shift saturates near 30 K at 2.2 kOe and additional magnetostatic modes become excited, which are visible as a couple of weaker lines on the right hand wing of the main resonance which is still well described by a Lorentz curve. The existence of the magnetostatic modes corroborates the presence of strong FM correlations. The width of the main resonance exhibits another minimum of 63 Oe at 38 K, due to suppression of the FM fluctuations, but then strongly broadens indicating spin fluctuations related to the transition into the noncollinear state. At 22 K a second weak resonancelike feature appears at low fields (marked by an arrow in Fig. 7) which on cooling continuously shifts to higher fields. Concomitantly the main resonance loses its Lorentzian shape and becomes heavily distorted, when merging with magnetostatic modes ( $T = 18$  K). Then both resonances overlap ( $T = 13$  K) and still deviate from Lorentzian shape. But finally, they separate again into two independent broad lines, one Lorentzian at low resonance field (1.5 kOe) and the second with irregular substructure at higher fields. At the same time the spectrum starts to reveal cubic anisotropy. Comparison with our magnetization data allows for identifying the small resonancelike

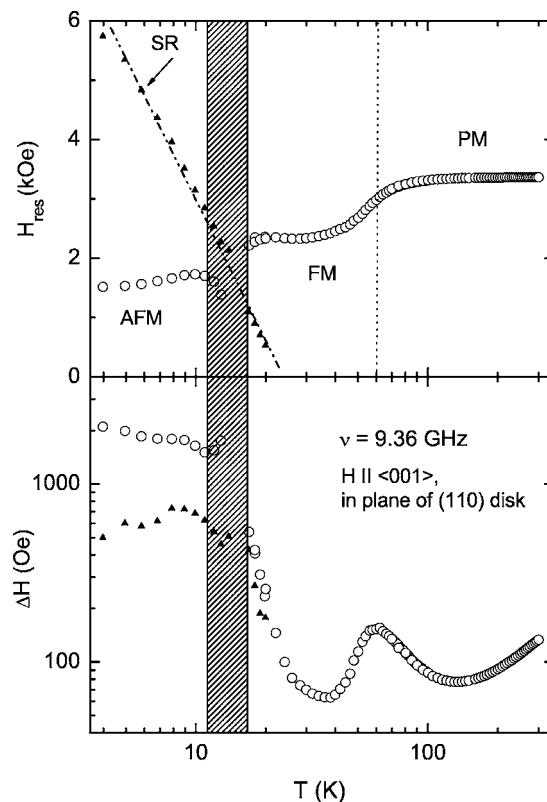


FIG. 8. Temperature dependences of the resonance field  $H_{\text{res}}$  (a) and linewidth  $\Delta H$  (b) for a thin  $\text{HgCr}_2\text{S}_4$  single crystalline disk with (110) plane orientation. Open circles indicate the main resonance in the paramagnetic (PM), ferromagnetic (FM), and antiferromagnetic (AFM) states. The solid triangles mark the resonance at the spin reorientation (SR).

feature which appears at 22 K with the transition into the noncollinear low-field magnetic phase. The reorientation of the magnetization at a certain field gives rise to an ESR signal in analogy to the spin-flop transition in conventional antiferromagnets. As long as this spin-flop like transition is at lower fields than the main resonance, this main resonance is characterized as a FM resonance because it originates entirely from the phase with FM correlations. On decreasing temperature the transition crosses the main resonance, i.e., at low fields the resonance features of the noncollinear phase appear, whereas at high fields the signal still has the FM character. In this temperature regime the spectrum is difficult to fit by a single line, and hence it is marked by the dashed area in Fig. 8. At temperatures below the crossover only the resonance of the noncollinear phase remains together with the spin-reorientation signal at high fields. The substructure and the quite large width of the high-field signal reflect the gradual change of the magnetization from the spiral into the FM structure found both in the specific heat and magnetization.

#### IV. CONCLUDING REMARKS

Our studies of the frustrated antiferromagnetic spinel  $\text{HgCr}_2\text{S}_4$  reveal unconventional behavior of the magnetic

properties and specific heat. The ground state is extremely sensitive to external fields. The noncollinear AFM spin configuration established below 22 K is suppressed by fields as low as 8 kOe. Moreover, the anomaly in the specific heat related to the AFM transition is characterized by a very low entropy contribution of the order of 1% of the full magnetic entropy. The magnetization and ESR measurements clearly evidence the appearance of strong ferromagnetic correlations below 50 K. At the same time, no conventional long-range FM order sets in and, respectively, no anomaly in the specific heat at the supposed FM transition is present.

Keeping in mind the peculiar arrangement of the Cr ions forming a corner-sharing tetrahedral network one may attribute the anomalous properties of  $\text{HgCr}_2\text{S}_4$  to geometrical frustration. However, the frustration parameter  $f$  (defined as the ratio of the Curie-Weiss temperature  $\Theta_{\text{CW}}$  to the Néel temperature  $T_N$ ) of about 6 for  $\text{HgCr}_2\text{S}_4$  is well below the limit of 10 usually taken to characterize geometrically frustrated magnets.<sup>21</sup> In addition, geometrical frustration occurs in systems dominated by AFM exchange, i.e., characterized by negative CW temperatures. The frustration parameter of the related sulfide spinel  $\text{ZnCr}_2\text{S}_4$  is even lower (about 1), but a complex AFM spin arrangement similarly develops at low temperatures which is apparently connected with strong magnetic frustration.<sup>29</sup> Geometrical frustration dominates in the oxide spinels, e.g.,  $\text{ZnCr}_2\text{O}_4$  and  $\text{CdCr}_2\text{O}_4$ , where it is linked to strong direct AFM exchange.<sup>30,31</sup> It seems to be less effective in the AFM sulfide spinels. As we already mentioned, in  $\text{HgCr}_2\text{S}_4$  the direct AFM exchange is considerably reduced in favor of large ferromagnetic NN superexchange due to the larger interatomic distance and results from the positive CW temperature of  $\text{HgCr}_2\text{S}_4$  ( $\Theta_{\text{CW}} = +140$  K) compared to  $\text{ZnCr}_2\text{O}_4$  ( $\Theta_{\text{CW}} = -390$  K). Our results suggest that bond frustration due to competing NN and NNN interactions governs the properties of  $\text{HgCr}_2\text{S}_4$ . It is important to note that in contrast to  $\text{HgCr}_2\text{S}_4$ , the other sulfide spinel,  $\text{CdCr}_2\text{S}_4$ , shows purely FM properties below the ordering temperature of 85 K, although it has just the same distance between the magnetic cations as  $\text{HgCr}_2\text{S}_4$  and only a slightly larger CW temperature ( $\Theta_{\text{CW}} = 152$  K). At first sight, it is quite surprising that this insignificant difference in the relative strength of competing interactions should be responsible for the high frustration in  $\text{HgCr}_2\text{S}_4$ . But comparing the ferromagnetic and antiferromagnetic exchange constants for these two com-

pounds, as estimated in Ref. 3 within mean-field approximation, we find a difference of about 1 K for the FM and of 0.3 K for the AFM exchange. This corresponds well to the Zeeman energy necessary to suppress the spiral structure in  $\text{HgCr}_2\text{S}_4$ . Thus far, a self-consistent model of the exchange interactions in this group of magnetic compounds is absent. The other type of interactions beside the direct exchange and superexchange might also be important, e.g., a biquadratic exchange as proposed by Grimes and Isaac.<sup>32</sup> Enhanced values of the sulfur positional parameter together with a very high value of the temperature factors in  $\text{HgCr}_2\text{S}_4$  (see Table I) suggest a possible off-center displacement of the octahedral Cr ions. In this case the biquadratic exchange can be considerably enhanced at low temperatures.<sup>32</sup> It can additionally contribute to bond frustration, which to our opinion is responsible for the unusual ground state in  $\text{HgCr}_2\text{S}_4$ .

In summary, structural, magnetization, electron-spin resonance, and specific heat studies have been performed on  $\text{HgCr}_2\text{S}_4$  polycrystals and single crystals. The high values of the atomic displacements suggest the proximity to a structural instability. Ferromagnetic correlations appear below 60 K and are strongly enhanced by the magnetic field. However, no conventional long-range FM order is established. The anomalies in the susceptibility and specific heat at 22 K are ascribed to a transition into an AFM state. Moderate magnetic fields (<5 kOe) reduce the anomaly in the specific heat and shift it to lower temperatures while higher fields completely suppress this anomaly. A ferromagnetic spin-wave contribution to the specific heat is evidenced at low temperatures. Above 22 K the electron-spin resonance reveals a narrow isotropic line due to FM correlations. Below 22 K the spectrum transforms into a broad line associated with the AFM correlations and a second line indicating a spin reorientation. The strong bond frustration due to competing exchange interactions between the Cr ions is suggested to be responsible for the observed anomalies in the magnetic properties and specific heat.

#### ACKNOWLEDGMENTS

This work was supported by the Deutsche Forschungsgemeinschaft via the Sonderforschungsbereich 484 (Augsburg) and partly by BMBF via VDI/EKM, FKZ 13N6917-B. The support of U.S. CRDF and MRDA via Grant No. MOP2-3050 is gratefully acknowledged.

<sup>1</sup>D. G. Wickham and J. B. Goodenough, Phys. Rev. **115**, 1156 (1959).

<sup>2</sup>F. K. Lotgering, *Proceedings of the International Conference on Magnetism*, Nottingham, 1964 (The Institute of Physics and the Physical Society, London, 1965), p. 533.

<sup>3</sup>P. K. Baltzer, P. J. Wojtowicz, M. Robbins, and E. Lopatin, Phys. Rev. **151**, 367 (1966).

<sup>4</sup>K. Dwight and N. Menyuk, Phys. Rev. **163**, 435 (1967); J. Appl. Phys. **39**, 660 (1968).

<sup>5</sup>S. Kondo, D. C. Johnston, C. A. Swenson, F. Borsa, A. V. Ma-

hajan, L. L. Miller, T. Gu, A. I. Goldman, M. B. Maple, D. A. Gajewski, E. J. Freeman, N. R. Dilley, R. P. Dickey, J. Merrin, K. Kojima, G. M. Luke, Y. J. Uemura, O. Chmaissem, and J. D. Jorgensen, Phys. Rev. Lett. **78**, 3729 (1997).

<sup>6</sup>A. Krimmel, A. Loidl, M. Klemm, S. Horn, and H. Schober, Phys. Rev. Lett. **82**, 2919 (1999).

<sup>7</sup>C. Urano, M. Nohara, S. Kondo, F. Sakai, H. Takagi, T. Shiraki, and T. Okubo, Phys. Rev. Lett. **85**, 1052 (2000).

<sup>8</sup>P. G. Radaelli, Y. Horibe, M. Gutmann, H. Ishibashi, C. Chen, R. Ibberson, Y. Koyama, Y.-S. Hor, V. Kiryukhin, and S.-W.

- Cheong, *Nature (London)* **416**, 155 (2002).
- <sup>9</sup>M. Schmidt, W. Ratcliff II, P. G. Radaelli, K. Refson, N. M. Harrison, and S. W. Cheong, *Phys. Rev. Lett.* **92**, 056402 (2004).
- <sup>10</sup>S.-H. Lee, C. Broholm, W. Ratcliff II, G. Gasparovic, Q. Huang, T. H. Kim, and S.-W. Cheong, *Nature (London)* **418**, 856 (2002).
- <sup>11</sup>V. Fritsch, J. Hemberger, N. Büttgen, E.-W. Scheidt, H.-A. Krug von Nidda, A. Loidl, and V. Tsurkan, *Phys. Rev. Lett.* **92**, 116401 (2004).
- <sup>12</sup>A. Krimmel, M. Mücksch, V. Tsurkan, M. M. Koza, H. Mutka, and A. Loidl, *Phys. Rev. Lett.* **94**, 237402 (2005).
- <sup>13</sup>N. Büttgen, J. Hemberger, V. Fritsch, A. Krimmel, M. Mücksch, H.-A. Krug von Nidda, P. Lunkenheimer, R. Fichtl, V. Tsurkan, and A. Loidl, *New J. Phys.* **6**, 191 (2004).
- <sup>14</sup>R. Fichtl, V. Tsurkan, P. Lunkenheimer, J. Hemberger, V. Fritsch, H.-A. Krug von Nidda, E.-W. Scheidt, and A. Loidl, *Phys. Rev. Lett.* **94**, 027601 (2005).
- <sup>15</sup>J. Hemberger, P. Lunkenheimer, R. Fichtl, H.-A. Krug von Nidda, V. Tsurkan, and A. Loidl, *Nature (London)* **434**, 364 (2005).
- <sup>16</sup>S. Weber, P. Lunkenheimer, R. Fichtl, J. Hemberger, V. Tsurkan, and A. Loidl, *Phys. Rev. Lett.* **96**, 157202 (2006).
- <sup>17</sup>R. P. van Stapele, in *Ferromagnetic Materials*, edited by E. P. Wohlfarth (North-Holland, Amsterdam, 1982), Vol. 3, p. 603.
- <sup>18</sup>J. M. Hasting and L. M. Corliss, *J. Phys. Chem. Solids* **29**, 9 (1968).
- <sup>19</sup>H. W. Lehmann and G. Harbeke, *Phys. Rev. B* **1**, 319 (1970).
- <sup>20</sup>P. W. Anderson, *Phys. Rev.* **102**, 1008 (1956).
- <sup>21</sup>A. P. Ramirez, in *Handbook of Magnetic Materials*, edited by K. H. J. Buschow (Elsevier Science, Amsterdam, 2001), Vol. 13, p. 423.
- <sup>22</sup>J. Rodriguez-Carvajal, *Physica B* **192**, 55 (1993).
- <sup>23</sup>N. W. Grimes, *Philos. Mag.* **25**, 1217 (1972).
- <sup>24</sup>J. Skalyo, A. F. Cohen, S. A. Friedberg, and R. B. Griffiths, *Phys. Rev.* **164**, 705 (1967).
- <sup>25</sup>T. A. Reichert, R. A. Butera, and E. J. Schiller, *Phys. Rev. B* **1**, 4446 (1970).
- <sup>26</sup>W. L. Johnson and W. Reese, *Phys. Rev. B* **2**, 1355 (1970).
- <sup>27</sup>A. Abragam and B. Bleaney, *Electron Paramagnetic Resonance of Transition Ions* (Dover, New York, 1986).
- <sup>28</sup>A. G. Gurevich and G. A. Melkov, *Magnetization Oscillations and Waves* (CRC Press, Boca Raton, Florida, 1996).
- <sup>29</sup>M. Hamedoun, A. Wiedenmann, J. L. Dormann, M. Nogues, and J. Rossat-Mignod, *J. Phys. Chem.* **19**, 1801 (1986).
- <sup>30</sup>H. Martinho, N. O. Moreno, J. A. Sanjurjo, C. Rettori, A. J. García-Adeva, D. L. Huber, S. B. Oseroff, W. Ratcliff II, S.-W. Cheong, P. G. Pagliuso, J. L. Sarrao, and G. B. Martins, *Phys. Rev. B* **64**, 024408 (2001).
- <sup>31</sup>M. T. Rovers, P. P. Kyriakou, H. A. Dabkowska, G. M. Luke, M. I. Larkin, and A. T. Savici, *Phys. Rev. B* **66**, 174434 (2002).
- <sup>32</sup>N. W. Grimes and E. D. Isaac, *Philos. Mag.* **35**, 503 (1977).